

RESEARCH PAPER • OPEN ACCESS

Polypyrrole Based Molecularly Imprinted Polymer Platform for *Klebsiella pneumoniae* Detection

To cite this article: Roshni Sharma *et al* 2022 *ECS Sens. Plus* 1 010603

View the [article online](#) for updates and enhancements.

You may also like

- [Comparison of chitosan and SLN nano-delivery systems for antibacterial effect of cinnamon \(*Cinnamomum verum*\) oil against MDR *K. pneumoniae* and *E. coli*](#)
Masoumeh Rohani, Mehran Nemattalab, Mohammad Hedayati et al.
- [Influence of photodynamic action on pure and mixed cultures of gram-negative bacteria: related to growth mechanisms](#)
Rebeca V de Lima, Jennifer M Soares, Kate C Blanco et al.
- [Application of nanotechnology in antimicrobial finishing of biomedical textiles](#)
Andrea Zille, Luís Almeida, Teresa Amorim et al.



Polypyrrole Based Molecularly Imprinted Polymer Platform for *Klebsiella pneumonia* Detection

Roshni Sharma,¹ G. B. V. S. Lakshmi,¹  Anil Kumar,^{2,z} and Pratima Solanki^{1,*} 

¹Special Center for Nanoscience, Jawaharlal Nehru University, New Delhi 110067, India

²National Institute of Immunology, New Delhi 110067, India

The present work describes the synthesis of molecular imprinting polymer (MIP) and electrochemical sensing of *Klebsiella pneumonia* (*K. pneumonia*) bacteria by electrochemical technique. *K. pneumonia* has far reached ill effects on the human body, hence it is essential to monitor its levels. A MIP platform based on polypyrrole (PPy) was developed for electrochemical sensing of *K. pneumonia* to monitor its levels. The developed sensor has good sensitivity ($3 \mu\text{A ml CFU}\cdot\text{cm}^{-2}$), a low limit of detection (LOD) of $1.352 \text{ CFU ml}^{-1}$ in the linear detection range of 1 to 10^5 CFU per ml . The molecular imprinting was carried out by polymerization of pyrrole in the presence of *K. pneumonia* and then removed the bacteria by ultrasonication to obtain the MIP. The fabrication of electrodes is done by electrophoretic deposition (EPD) of MIP onto the hydrolyzed ITO-coated glass surface. The detection was done by the electrochemical differential pulse voltammetry (DPV) technique. The synthesized final product is then characterized by Fourier transform infrared spectroscopy (FTIR) technique to understand its structure and confirm the successful synthesis of the desired MIP. The selectivity studies were performed against two other bacteria and different ions that are present in healthy human urine. To check the applicability in real sample studies, spiked urine samples were used.

© 2022 The Author(s). Published on behalf of The Electrochemical Society by IOP Publishing Limited. This is an open access article distributed under the terms of the Creative Commons Attribution 4.0 License (CC BY, <http://creativecommons.org/licenses/by/4.0/>), which permits unrestricted reuse of the work in any medium, provided the original work is properly cited. [DOI: 10.1149/2754-2726/ac612c]



Manuscript submitted February 17, 2022; revised manuscript received March 25, 2022. Published April 13, 2022.

K. pneumonia is a well-known gram-negative type opportunistic pathogenic bacterium, belonging to *Klebsiella spp. K. pneumonia* and asymptotically colonize in the human intestine, skin, nose, and throat where they do not cause any disease.¹⁻³ It is mostly present in the hospital environment such as in hospitalized patients⁴⁻⁶ or in medical equipment such as bronchoscopy, duodenoscopy, gastroscopy in intensive care unit⁷⁻¹¹ etc. It is the main cause of nosocomial infection and is characterized by bloodstream infection, pneumonia, wound site infection, urinary tract infection,¹² sepsis, bacteremia,¹³ and peritonitis¹⁴ mostly in older adults, newborn infants, and immune-suppressed patients.^{15,16} Therefore, for controlling the spread of these pathogenic bacteria, its determination through rapid, sensitive and accurate identification method is required.¹⁷ The detection of *K. pneumonia* bacteria involves traditional microbial culture-based test,¹⁸ PCR,^{19,20} antibody-antigen interaction based techniques, and various analytical methods which are shown in Table I, but these methods require long incubation time, have complex and costly instrumentation and procedure, easy contamination possibility, and also, they are unable to provide the results in real-time which are the main limitations of these methods.

To overcome these issues, a rapid, inexpensive, simple technique with high selectivity and sensitivity to distinguish between closely related microorganisms must be developed for the detection of *K. pneumonia*. Different approaches are used for the recognition of the deliberation of the bacteria.²⁶⁻²⁹ MIP is one of the best effective alternative methods for the recognition of microorganisms with improved sensitivity and good selectivity because microorganisms having specific conformation and structure can be imprinted with functionally and sterically opposite places inside the MIP after the template removal. Besides the clearer identification features of MIPs, their chemical and physical characteristics are extremely alluring.³⁰ Because of their highly cross-linked nature, they show great stability, chemical and physical confrontation to various external harmful effects even in extreme conditions like high temperature, high pressure, mechanical stress and can be stored for long time periods. They can be used multiple times in excess with not damaging the “memory effect.” They possess readily template-specific, three-dimensional interaction sites inside the imprinted polymer.³¹⁻³³ The presence of cavities in the polymer matrix occurs due to the elimination of the template compound. There is particular bonding and structure for

the template molecule to maintain in the cavity form in the polymer so that the printed polymer selectively binds the template molecule. For the development of MIP mostly conducting polymers are used for entrapping the analyte as they possess good stability, electrochemical properties, easy synthesis, and sensitivity.³⁴

In this work, Polypyrrole (PPy) was used as the polymer matrix for developing MIP. For the development of the sensor, oxidative polymerization of pyrrole monomer in the presence of the template i.e., *K. pneumonia* was carried out followed by the removal of the template using sonication and washing with deionized water. The MIP electrode was electrophoretically deposited on ITO coated glass electrode. The sensing was done by the electrochemical sensing method and analyzed using cyclic voltammetry and DPV curves. The attained result of the study was compared with the literature given in Table I. Results show this method overcomes some of the disadvantages of previously reported techniques such as high incubation time with poor sensitivity range, complex procedure, and more time consuming as compared to the sensor developed with the MIP method. Though, there is not a single report that exists on the PPy-based MIP system for detecting *K. pneumonia*. Therefore, there is a broad scope to develop a MIP-based sensing platform for the detection of *K. pneumonia*.

Experimental

Materials.—Pyrrole (98%; purchased from Sigma Aldrich), hydrochloric acid (HCl), and chloroform 99.5% (both purchased from Qualigens) were used for the synthesis of PPy. Propane 2-ol (99.7%; fisher scientific), acetonitrile (99.9%; Thomas baker), and anhydrous ferric chloride (FeCl_3) (98%; HI media) were used in this procedure. HCl, potassium ferrocyanide ($\text{K}_4[\text{Fe}(\text{CN})_6]$), potassium ferricyanide ($\text{K}_3[\text{Fe}(\text{CN})_6]$), sodium phosphate dibasic dehydrate (Na_2HPO_4), and sodium phosphate monobasic dehydrate (NaH_2PO_4) were obtained from Fisher Scientific. All the solutions were prepared in DI water obtained from the Millipore water purification system. Indium tin oxide (ITO) coated glass with 1.1 mm thickness and sheet resistance of 25 ohm cm^{-2} purchased from Blazers (U.K) having a transmittance of 90%. For the electrochemical response study, the bacterial concentrations of different CFU values (1–10,000 CFU) were prepared.

Bacterial culture preparation.—All cell strains were cultured on Mueller-Hinton (MH) agar plate at 37°C in an incubator. Before the

*Electrochemical Society Member.

^zE-mail: anilk@nii.ac.in; partima@mail.jnu.ac.in

Table I. Comparative table of different methods used for the detection of *K. pneumoniae*.

Methods	Techniques	Electrode	Linear range	LOD	Sensitivity	Response time	References
LFTS assay	—	a glass fiber pad	10^3 – 10^7 CFU	—	$> 10^4$ CFU	15 min	21
ISFET sensors	pH meter	CMOS-based Lab-on-Chip platform	10 – 10^5 CFU	—	—		22
real-time PCR	—	—	10 – 10^7 CFU		10^3 CFU	40 min	23
Electrochemical Biosensor	DPV	Glass carbon electrode	10^5 – 10^8 CFU	10^7 CFU			24
Electrochemical Biosensor	CV, DPV	graphene electrode	3.4×10^3 CFU– 3×10^7 CFU	3×10^7 CFU	10^7 CFU	60 min	25

experiment, the primary and secondary cultures were prepared. For primary culture, a single colony of bacteria was added to 5 ml of broth media and left in an incubator at 37 °C for 24 h. For secondary culture, 50 μ l of primary culture is added into 5 ml of media and left for 3 and a half hrs in the incubator at 37 °C. This fresh culture was rinsed three times using PBS by centrifuging at 5000 rpm and 4 °C. OD 600 was used to measure the cell density in a suspension.

Synthesis of MIP.—The synthesis of MIP of *K. pneumonia* was done by the interfacial oxidative polymerization process by using ferric chloride as an oxidizing agent. For this process two solutions are prepared in different beakers, first one is 50 mM ferric chloride solution (200 ml) containing 1 M HCl (20 ml) in which 1 ml of 0.5 OD *K. pneumonia* bacterial cells are added to it (known as aqueous phase) and the second one is 1 M pyrrole added in 20 ml chloroform (known as organic phase). For the interfacial polymerization, these two solutions were mixed carefully and slowly by transferring the aqueous phase solution in the beaker having pyrrole monomer solution along the sidewalls of the beaker and kept undisturbed for 24 h at room temperature. After 24 h, the PPy polymer layer was formed in between the oil and aqueous phases. The oil and aqueous phases were pipetted out slowly and carefully to collect the PPy polymer containing *K. pneumonia* cells. The unreactive residue of pyrrole monomeric units and oxidant were removed by washing the precipitate with DI and ethanol simultaneously and the washed polymer was collected by filtration. The collected filtrate was divided into two parts: the first part was dried and stored as it is without any further washing and named as NIP + *K. pneumonia* and another part was sonicated for 12 h continuously followed by centrifugation at 5000 rpm for 20 min, washed with DI water and dried at 60 °C overnight which was named as MIP. For the synthesis of non-imprinted polymer (NIP) all the above steps were kept the same except the addition of *K. pneumonia* cells. The final products MIP and NIP were characterized by FTIR. For the electrode fabrication by electrophoretic deposition-1 mg of MIP, NIP, and NIP + *K. pneumonia* in 500 μ l of isopropyl alcohol and 500 μ l of acetonitrile was taken in different vials and sonicated for 4 h. The schematic diagram (Scheme 1) shows the overall synthesis and identification of bacteria based on MIP.

Fabrication of electrode.—For the fabrication of electrodes via EPD method ITO coated glass of 1.5 cm \times 0.5 cm was used. For this acetonitrile was used as an electrolyte or conducting liquid. The ITO

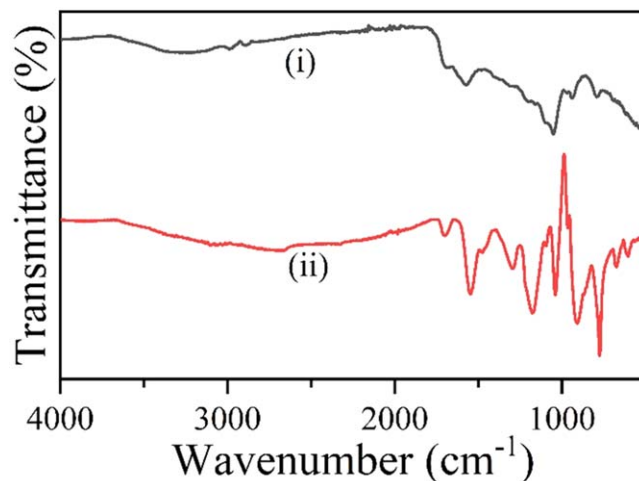


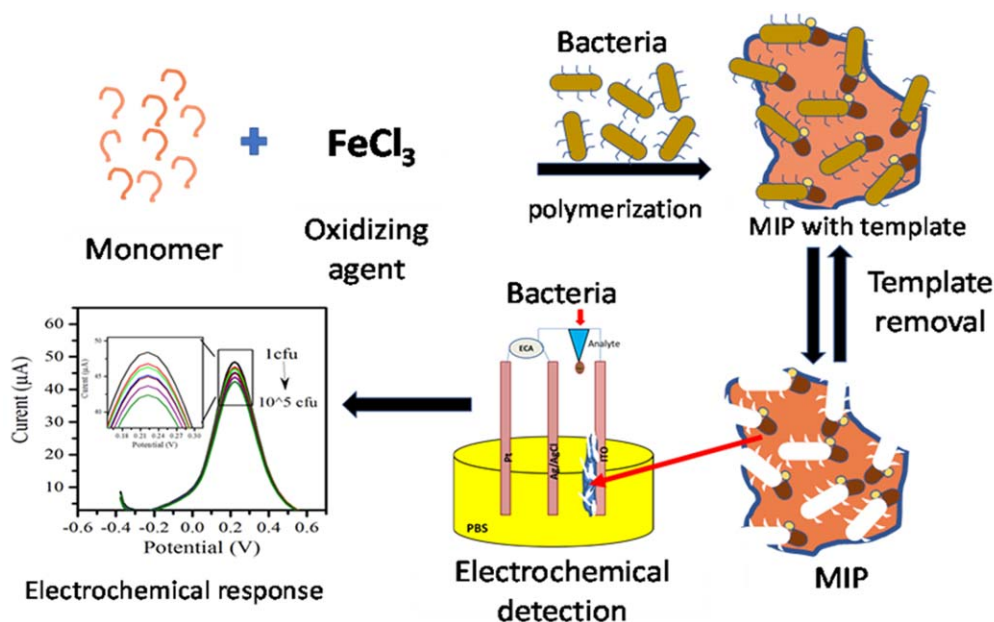
Figure 1. FTIR spectra of (i) NIP and (ii) MIP.

glass sheet was cleaned with ethyl alcohol and DI water, and hydrolyzed these sheets by taking H₂O₂, NH₃, and water solution in 1:1:5 volume ratios and placing the sheets in this solution at 70 °C for 1 h and dried at room temperature. For electrophoretic deposition of the electrode, dispersion of MIP, NIP was done in acetonitrile with Mg ion used as a catalyst. For an electrochemical reaction, a voltage of 50 V was applied. Due to the difference in potential between electrodes, ions created at the electrode migrated to the oppositely charged electrode, and the film was deposited on the ITO-coated glass sheet. The schematic diagram (Scheme 1) shows the overall synthesis and identification of bacteria based on MIP.

Results and Discussion

Fourier transformation infrared spectra (FT-IR) study.

Figure 1 shows the FTIR spectrum of NIP and MIP samples. There are changes in the bond vibrations observed in MIP as compared to NIP as follows. In NIP the occurrence of a weak peak at 3400 cm⁻¹ is assigned to the presence of N–H stretching vibrations of the pyrrole ring. The weak band at 1800 cm⁻¹ is due to C–H stretching. The characteristic peak at 1600 cm⁻¹ corresponds to the C=C stretching and the peak at 1100 cm⁻¹ is due to C–C stretching



Scheme 1. Schematic representation of the MIP formation and electrochemical response.

confirming the formation of PPy.³⁵ The FTIR spectra of MIP samples after removing bacterial cells are recorded the same as in NIP in the range of 4000 to 500 cm^{-1} to confirm polymerization. All the peaks that are of NIP are matching in both cases. Although the peak positions are the same, there is a change in shape and intensity was observed. There are few extra peaks are also observed due to the interaction between PPy and lipopolysaccharide, peptide bonds present in the outer membrane of the bacterial cell. The peak we get around at 900 cm^{-1} , 1000 cm^{-1} and 1100 cm^{-1} which are due to C–H stretching and CH out of plane deformation, vinyl indene bond stretching, CN stretching in aromatic rings, and phosphorous oxy acids respectively, which were of few bacterial cells remained in MIP after removal.

Electrochemical study

Electrochemical behavior of MIP (*K. pneumonia*)/ITO electrode at different pH of PBS solution.—The pH value has a significant role in the electrochemical reaction between the analyte and electrode. Therefore, 0.2 mM PBS buffer solution having $[\text{Fe}(\text{CN})_6]^{3-/4-}$ redox species at different pH values varying from 6 to 8 pH was used to see the effect of pH by the DPV curve in the potential range from -0.8 to 0.8 on MIP/ITO electrode. As shown in Fig. 2a, the peak current changes with the change in pH value. More specifically, the electrochemical response of MIP gradually decreased as the pH increased from 6.5 to 7.4 and then increased to pH 8.0. This study showed that *K. pneumonia* cells (0.05 OD) interact more with imprinted cavities at pH 8.0 by showing higher DPV peak current values. Therefore, pH 8.0 buffer was used for further observations.

Response time study.—The time required to bind the analyte molecule with the MIP surface depends on the incubation time. It has an important role in the performance of the sensor. Therefore, response time studies were analyzed by using DPV curve within the time interval 0 to 12 min, and the peak currents are plotted in Fig. 2b. This study was carried out with *K. pneumonia* bacteria cell (0.05 OD) added to the buffer in an electrochemical cell containing MIP and the DPV peak current was noted after every 3 min. It was observed that the peak current decreased at 3 min and later there is no significant change in the current. Therefore, it was concluded that approx. 3 min is required for the interaction of the bacterial cell with the MIP electrode. Thus, every reading of the response study after introducing the bacterial cell was taken after 3 min.

Electrode study and scan rate.—To analyze the electroactivity of NIP + bacteria/ITO, MIP/ITO, and NIP/ITO electrodes, the CV (at scan rate 50 mV s^{-1}) and DPV studies in the potential range of -0.4 V to 0.6 V were carried out. Figures 3a and 3b showed the CV

and DPV current response of (i) NIP + bacteria/ITO, (ii) NIP/ITO and (iii) MIP/ITO electrodes. It was observed that the peak current of NIP/ITO and NIP with bacteria/ITO have almost the same current with a slight increase in the peak voltage. Whereas, in MIP (iii), the peak current was increased. It was observed that the current increased drastically for MIP/ITO electrode after the bacterial cell was removed from the polymer matrix by simply washing and ultrasonication. This may be due to the formation of cavities on PPy after the removal of bacterial cells. So, the electroactivity of the electrode increased and thereby increasing the CV and DPV peak currents of MIP. These changes in the peak current and FTIR study showed that bacterial cell was successfully removed from the polymer matrix in MIP.

The electrokinetics behavior of MIP/ITO electrodes was analyzed by the CV study by changing the scan rate from 10 to 100 mV s^{-1} . This study gives an idea about the kinetics of the reaction which occurs at the interface of the electrode and electrolyte solution (Fig. 3c). Between the peak current I_{pa} (anodic) and I_{pc} (cathodic) to the square root of \sqrt{v} there is a linear relationship observed as shown in the inset of Fig. 3c which indicates the diffusion-controlled electrochemical process which depends on the diffusion of electrolyte species.^{36,37}

The I_{pa}/I_{pc} ratio of the MIP electrode was found to be 0.80 indicating the irreversible electron transfer kinetics for MIP/ITO electrode^{36,38} in the medium. The interface kinetic parameters of the electrodes such as surface area (A_e), the electron transfer coefficient (Ks) [calculated using Eq. 1], the surface concentration of adsorbed electroactive species (γ^*) [calculated using Eq. 2], Diffusion coefficient (D) [calculated using Eq. 3], were estimated to analyze the movement of electrons. The Randles-Sevcik equation (Eq. 3) determined the diffusion coefficient (D) as mentioned in the study of Lakshmi et al.³⁹

$$K_s = mnFV/RT \quad [1]$$

$$\gamma^* = 4RTI_a / n^2F^2AV \quad [2]$$

$$D = I_a^2 / (2.99 \times 10^5)^2 A^2 n^3 C^2 V \quad [3]$$

Where $n = 1$ for ferri-ferro buffer, $F = 96485$, $R = 8.314$, $T = 300$ K, $V = 50$ mV s^{-1} .

$C =$ concentration of buffer = 0.1 M.

$A =$ area of the electrode.

$m = E_a - E_c$.

The obtained values are $K_s = 0.519$, $\gamma^* = 1.734 \times 10^{-8}$, $D = 1.46 \times 10^{-12}$. The results show that there exists good conductivity for charge transfer between the electrolyte and the electrode.

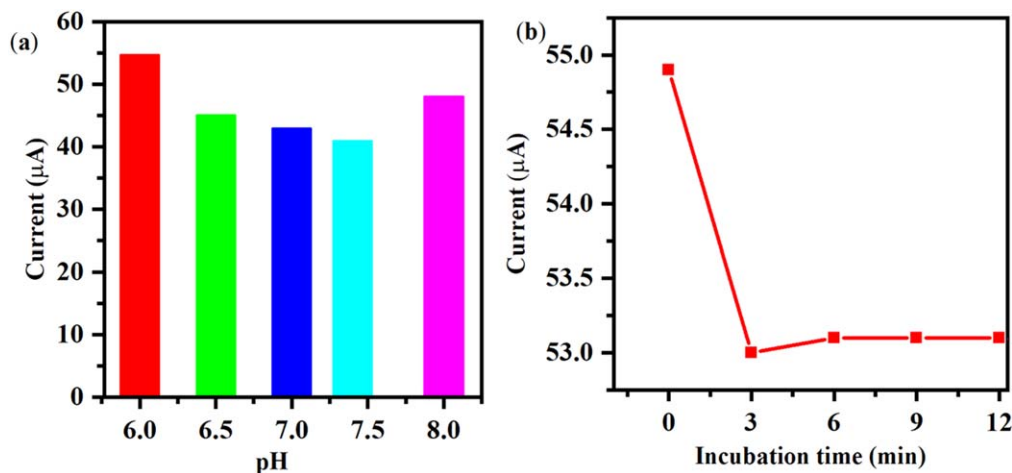


Figure 2. Electrochemical study of MIP electrode: (a) effect of pH. (b) Incubation time/response time study.

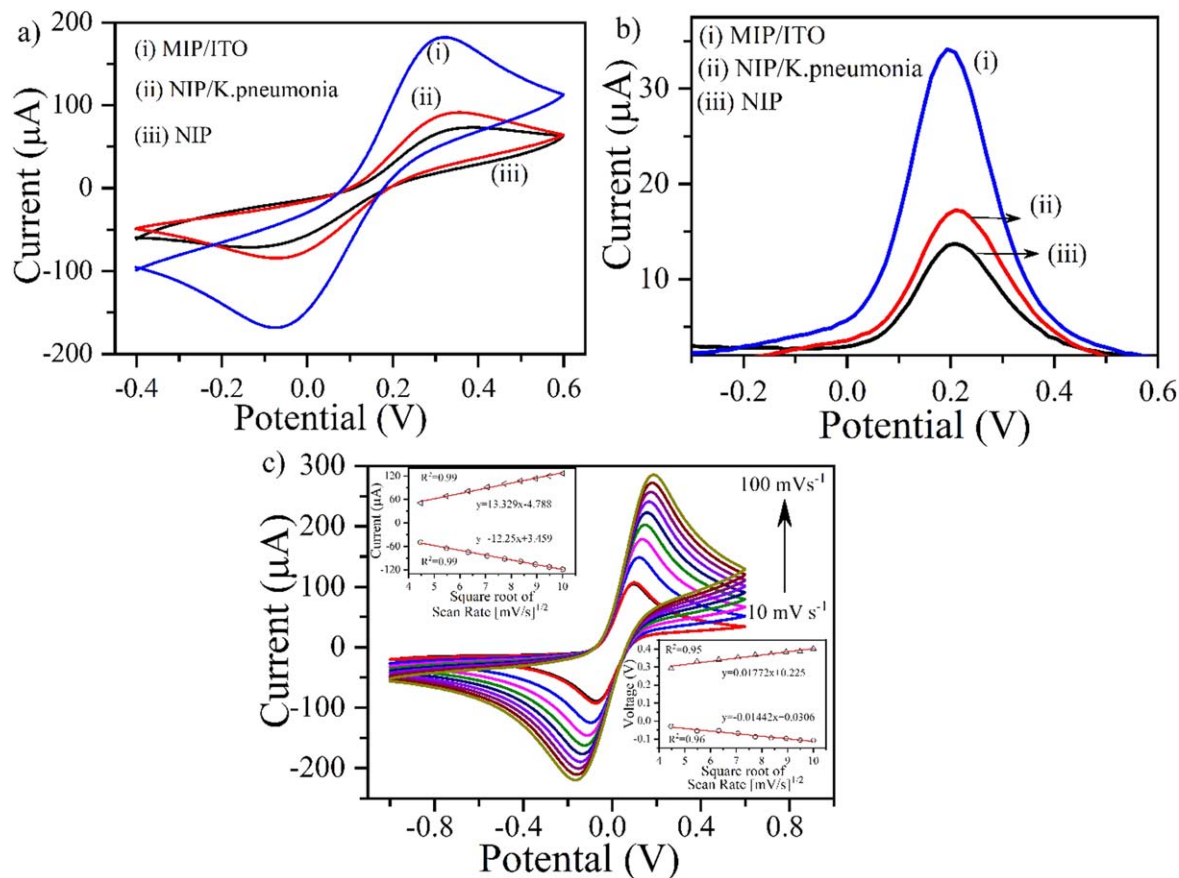


Figure 3. (a) Comparative CV and (b) DPV study of: (i) NIP + bacteria/ITO electrode, (ii) NIP/ITO electrode and (iii) MIP/ITO electrode. (c) CV curve of MIP/ITO electrode at a and different scanning rates (10–100 mV s⁻¹) in PBS buffer (pH 8) containing 5 mM ferri/ferro mediator. Inset (c) shows the peak current (I_{pa} and I_{pc}) with \sqrt{v} (top) and peak potentials with \sqrt{v} (bottom).

Electrochemical Response Study

For the analysis of the electrochemical response, DPV is the more suitable technique than CV because it has higher sensitivity. Therefore, for the sensing of analyte (*K. pneumoniae* bacteria), the DPV technique was conducted on MIP/ITO electrode in the potential range from -0.4 to 0.6 V at various concentrations of bacteria cells from 1 CFU to 10⁵CFU (1, 10, 100, 1000, 10⁴, 10⁵ CFU) with 3 min incubation time at room temperature. From Fig. 4 (enlarge peak position in inset of Fig. 4a), it was observed that as the concentration of bacterial cells increased from 1 to 10⁵ CFU, the peak current decreased linearly and became constant (no change) after adding 10⁵ CFU bacterial concentration. Hence, the 10⁵ CFU concentration was the saturation concentration because above this concentration cavities on the MIP electrode were saturated and no further decrease in current was observed. Also, the lowest limit of detection is 1 CFU for the developed sensor. Figure 4b showed the calibration curve with an error bar between the different concentrations of *K. pneumoniae* and the change in DPV peak current of MIP/ITO. The sensitivity was calculated using the slope of the calibration plot/area of the working electrode as 3 $\mu\text{A ml}^{-1}$ CFU cm⁻². The limit of detection was calculated using $3\sigma/\text{slope}$ of the calibration plot as 1 CFU ml⁻¹, where “ σ ” is the standard deviation of the intercept.

These results show that the detection of *K. pneumoniae* bacteria using this method is useful and better than other methods as mentioned in Table I. The PPy prepared by oxidative polymerization reaction has a positive charge along the polymer backbone, which has the ability to entrap negatively charged bacteria from polymeric film.⁴⁰ Gram-negative bacteria have lipid, a thin layer of peptidoglycan, lipid-protein bilayer in the outer membrane cell wall that helps in the binding. So basically, the membrane contains proteins,

phospholipids, and lipopolysaccharides.⁴¹ This lipopolysaccharide contains more charge per unit surface area than any phospholipids due to the exposure of the carboxyl groups and phosphoric groups which are readily ionized. So, this charge becomes anionic at a slightly basic pH 8. Therefore, this outer membrane face of a bacterial cell is highly charged, and additionally, the most necessary property is the polymer backbone has a positive charge which recompenses to the anionic molecule in the structure.⁴² Carboxylic, hydroxyl, and phosphate are anionic functional groups that are exposed to the outer cell membrane of gram-negative bacteria. Thus, positive charge containing polymer entrapped bacterial cell through hydrogen, Vander Waals forces and dipole-dipole interactions and hydrophobic interactions.⁴³ As these are weak interaction forces, the template could be removed by ultrasonication for template-free recognition site produced. When different bacterial concentrations were added, the bacterial cells started interacting with PPy film, so the electroactivity, as well as DPV peak current, decreased.

Both values are practically good and show the precision of the consistency and accuracy of the sensor for real-time diagnosis. In view of the fact that *K. pneumoniae* bacteria are present in the urine, the spiked detection in urine samples by this sensor will be helpful.

Control Study

This study shows the electrochemical behavior of NIP/ITO at different OD (CFU) of bacterial cells and confirms the lack of the reactivity of NIP electrodes with bacteria. As there are no specific cavities present in NIP, it did not interact with the bacterial cell. Figure 5a shows that as the CFU concentration increases, there is no significant change in the DPV current of the NIP/ITO electrode. This proved that on the MIP electrode surface, specific interaction was

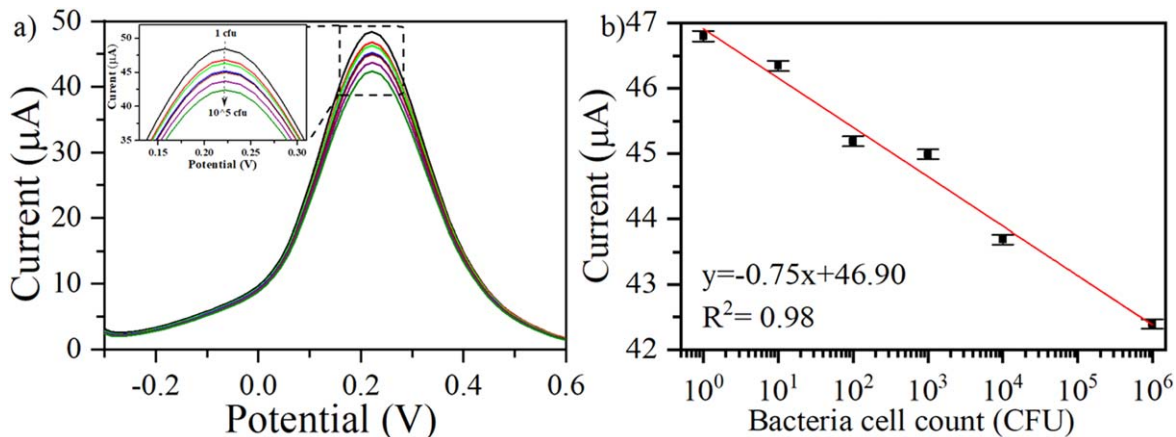


Figure 4. (a) DPV current response of MIP/ITO electrode as a function of bacterial cell amount (1 to 10^5 CFU) (magnified view of peak current in inset). (b) Calibration curve of the peak current with bacterial cell count (CFU) ($\text{mL CFU}^{-1}\text{cm}^{-2}$).

involved between the *K. pneumonia* and imprinted active sites (cavities).

Interference Study

Interference study gives an idea about the specificity of the sensor which is an important and essential parameter to define the performance as well as the characteristics of the sensor. For this, different elements of human urine such as uric acid [0.03 g per ml], potassium ions (K^+) [0.25 g per 100 ml], magnesium ion (Mg^{++}) [0.015 g per ml], urea [2 g per 100 ml] were used as interferences. Also, other bacteria cells of *Lactobacillus* and *E. coli* (10 CFU each) were also tested for interference. Figure 5b shows the DPV peak

current of MIP/ITO electrode with different interferences. As the various interferences are added into the electrolyte, there is no significant change in peak current observed. But upon adding the 10 CFU *K. pneumonia* cells, the current decreased to $33 \mu\text{A}$, with the highest difference from that of other components, indicating that the *K. pneumonia* cells are specifically interacting with the MIP/ITO.

Spiked Sample Study

For this study, a healthy human urine sample was collected and spiked with *K. pneumonia* at different concentrations as used in the response study. The spiked urine samples ($20 \mu\text{l}$ each) were added to the electrochemical cell and the DPV peak current was noted at each

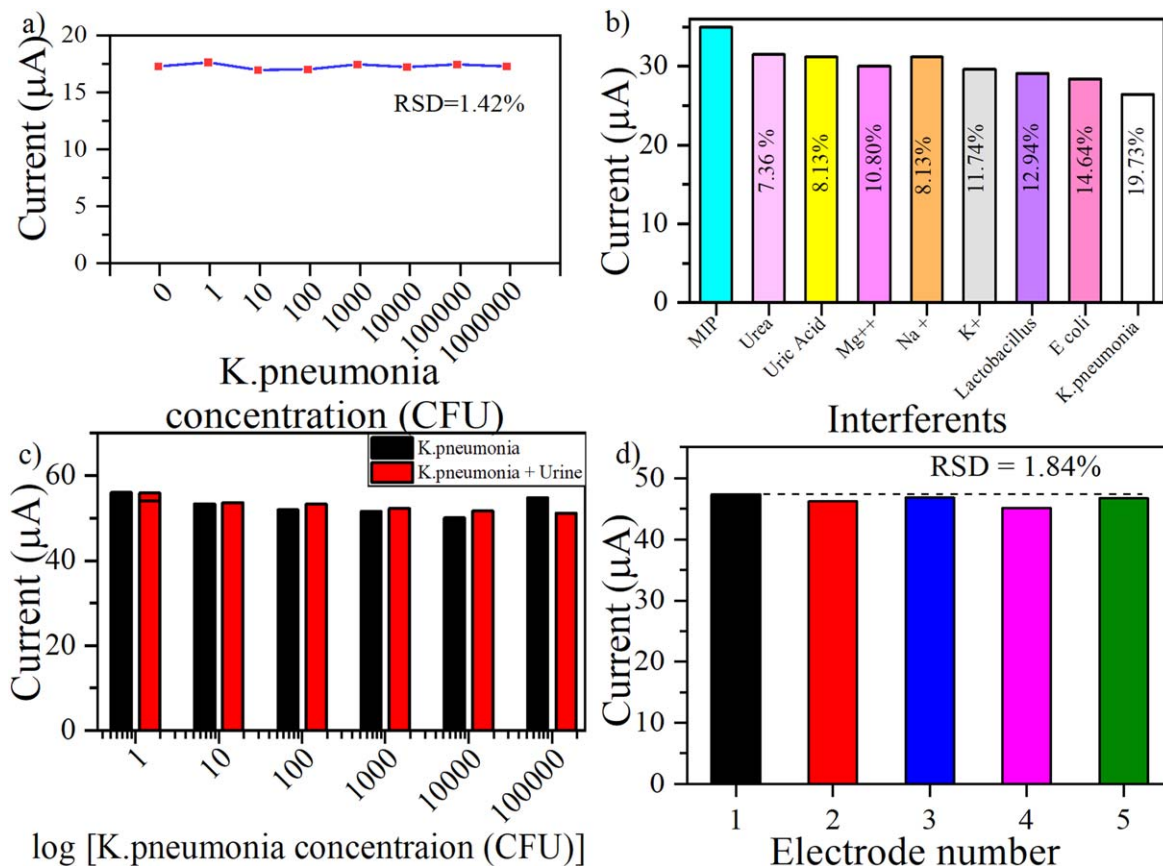


Figure 5. (a) Control study in NIP/ITO electrode via DPV peak current V/s bacterial concentration (1 to 10^5 CFU ml^{-1}). (b) Interferents response on MIP/ITO electrode. (c) Comparison of Spiked in peak current in MIP/ITO electrode with bacterial concentration. (d) Reproducibility study of MIP/ITO electrode.

Table II. Recovery percentage and RSD % (relative standard deviation) of *K. pneumonia*.

Bacterial cell added to the urine sample (CFU)	DPV peak current for sensing (μA)	DPV peak current for spiked sample (μA)	Relative standard deviation (RSD %)	Recovery (%)
0	56.065	55.942	0.16%	99.781
1	54.102	54.102	0%	100
10	53.366	53.612	0.33%	100.46
100	51.956	53.366	1.89%	102.69
1000	51.5880	52.262	0.92%	101.3
10000	50.115	51.772	2.30%	103.3
100000	54.852	51.158	4.93%	93.26

concentration (red) and plotted in comparison with response study values (black) as shown in Fig. 5c. As the concentration of bacteria (*K. pneumonia*) increased sequentially, the peak current decreased in spiked samples. From the known concentration of spiked *K. pneumonia* cells (1 to 10⁵ CFU per ml), the relative standard deviation (RSD) and the percent recovery were measured and shown in Table II.

Reproducibility Study

To assure the reproducibility of electrodes, the electrochemical behavior of five electrodes prepared in identical conditions with the similar total area was studied using DPV. Figure 5d shows the DPV peak current of different electrodes and found that, all electrodes have comparable current values with an RSD of 1.84% indicating the better reproducibility of the electrodes.

Conclusions

In the present study, MIP based electrochemical sensor for *K. pneumonia* bacteria detection was successfully fabricated for the first time using a conducting polymer polypyrrole (PPy). The MIP has complementary cavities against the imprinted bacteria. The synthesis of MIP has great attention due to the simple, cost-effective, biocompatibility of the polymer matrix. Due to oxidative polymerization reaction positively charged PPy formed along with the polymer backbone chain which easily captured the negatively charged bacteria inside polymeric film via electrostatic interaction which is a weak interaction. Therefore, bacteria were easily removed from the polymer matrix by ultra-sonication and then finally washed with ethanol and DI. The morphological and functional characterizations were performed by FTIR and DPV to check the incorporation and subsequent removal of bacteria. The fabrication of electrodes for the detection of *K. pneumonia* bacteria using the synthesized MIP was done by the electrophoretic deposition method. The developed MIP-based sensor showed excellent sensitivity of 3 $\mu\text{A ml CFU-cm}^{-2}$, LOD (limit of detection) 1.352 CFU ml⁻¹, linear detection range 1 to 10⁵ CFU per ml. The sensitivity of the present MIP may be further improved by changing the polymer monomers or by incorporating some nanomaterials into the MIP matrix.

Acknowledgments

The authors are thankful to Advanced Instrument Research Facility (AIRF), Jawaharlal Nehru University (JNU) for facilitating the instrumentation facility. GBVSL is thankful to DST for funding through DST Women Scientist Project. This work was supported by a grant (PAC-SCNS-PS-DBT-12151218-934) from the Department of Biotechnology, Government of India, India, and the Department of Science and Technology (DST), India.

ORCID

G. B. V. S. Lakshmi  <https://orcid.org/0000-0001-7055-4533>

Pratima Solanki  <https://orcid.org/0000-0003-1679-2180>

References

1. F. Kontopidou, H. Giamarellou, P. Katerelos, A. Maragos, I. Kioumis, and E. Trikka-Graphakos, *Clin Microbiol Infect.*, **20**, O117 (2014).

2. A. Kola, B. Piening, U.-F. Pape, W. Veltzke-Schlieker, M. Kaase, and C. Geffers, *Antimicrob Resist Infect Control.*, **4**, 122–4 (2015).
3. T. Naas, G. Cuzon, A. Babics, N. Fortineau, I. Boytchev, and F. Gayral, *J. Antimicrob. Chemother.*, **65**, 1305–6 (2010).
4. E. S. Snitkin, A. M. Zelazny, P. J. Thomas, F. Stock, D. K. Henderson, and T. N. Palmore, *Sci Transl Med.*, **4**, 148ra116 (2012).
5. A. Kola, B. Piening, U.-F. Pape, W. Veltzke-Schlieker, M. Kaase, and C. Geffers, *Antimicrob Resist Infect Control.*, **4** (2015).
6. T. Naas, G. Cuzon, A. Babics, N. Fortineau, I. Boytchev, and F. Gayral, *J. Antimicrob. Chemother.*, **65**, 1305–6 (2010).
7. E. S. Snitkin, A. M. Zelazny, P. J. Thomas, F. Stock, D. K. Henderson, and T. N. Palmore, *Sci. Transl. Med.*, **4**, 148ra116 (2012).
8. G. V. Sanchez, R. N. Master, R. B. Clark, M. Fyyaz, P. Duvvuri, and G. Ekta, *Emerg Infect Dis.*, **19**, 133–6 (2013).
9. G. Starlander and Å. Melhus, *J Hosp Infect.*, **82**, 122–4 (2012).
10. L. Niu, F. Zhao, J. Chen, J. Nong, C. Wang, J. Wang, and S. Hu, *PLoS One*, **13**, e0204332 (2018).
11. Y. Wang, W. Yan, Y. Wang, J. Xu, and C. Ye, *J. Microbiological Methods*, **149**, 80–8 (2018).
12. A. Khatri et al., *Antimicrob. Agents Chemother.*, **59**, 4375–8 (2015).
13. A. Togawa, H. Toh, K. Onozawa, M. Yoshimura, C. Tokushige, N. Shimono, T. Takata, and K. Tamura, *J. Infect. Chemother.*, **21**, 531–7 (2015).
14. M. J. Kim et al., (2014) *Hepatol. Int.*, **8**, 582–7.
15. H. Ariffin, P. Navaratnam, M. Mohamed, A. Arasu, W. A. Abdullah, C. L. Lee, and L. H. Peng, *Int. J. Infect. Dis.*, **4**, 21–5 (2000).
16. C. Hennequin and C. Forestier, *Res. Microbiol.*, **158**, 339–47 (2007).
17. Z. Zhang, H.-W. Yu, G.-C. Wan, J.-H. Jiang, N. Wang, Z.-Y. Liu, D. Chang, and H.-Z. Pan, *J. AOAC Int.*, **100**, 548–52.
18. O. Lazcka, F. J. Del Campo, and F. X. Muñoz, *Biosens. Bioelectron.*, **22**, 1205–17 (2007).
19. G. Cuzon, T. Nass, P. Bogaerts, Y. Glupczynski, and P. Nordmann, *Diagn. Microb. Infect. Dis.*, **76**, 502–5 (2013).
20. M. Hindiyeh et al., *J. Clin. Microbiol.*, **49**, 2480–4 (2011).
21. T. Tomimaga, *J. Microbiol. Methods*, **147**, 43–9.
22. J. Rodriguez-Manzano, N. Miscourides, K. Malpartida-Cardenas, I. Pennisi, N. Moser, A. Holmes, and P. Georgiou, [IEEE 2019 IEEE Biomedical Circuits and Systems Conference (BioCAS)-Nara, Japan (2019.10.17–2019.10.19)] 2019 IEEE Biomedical Circuits and Systems Conference (BioCAS) (2019).
23. P. Kurupati, C. Chow, G. Kumarasinghe, and C. L. Poh, *J. Clin. Microbiol.*, **42**, 1337–40 (2004).
24. H. Duyen Thi Ngoc, K.. Ah-Young, and K.. Young-Rok, *Sensors*, **17**, 1406 (2017).
25. M. K. Pachouri and M. Pankaj, *J. Chem. Sci.*, **5**, 88–97 (2015).
26. S. Pal and E. C. Alcocija, *Biosens. Bioelectron.*, **24**, 1437–44 (2009).
27. A. G. Gehring and S. I. Tu, *J. Food Prot.*, **68**, 146–9 (2005).
28. M. Ates, *Prog. Org. Coat.*, **71**, 1–10 (2011).
29. N. Jaffrezic-Renault, C. Martelet, Y. Chevolut, and J. P. Cloarec, *Sensors (Basel)*, **7**, 589–614 (2007).
30. H. Ariffin, P. Navaratnam, M. Mohamed, A. Arasu, W. A. Abdullah, C. L. Lee, and L. H. Peng, *Int. J. Infect. Dis.*, **4**, 21–5 (2000).
31. A. Mujahid, N. Iqbal, and A. Afzal, *Biotechnol. Adv.*, **31**, 1435–47 (2013).
32. P. A. Lieberzeit, S. Gazda-Miarecka, K. Halikias, C. Schirck, J. Kauling, and F. L. Dickert, *Sens. Actuators B Chem.*, **111**, 259–63 (2005).
33. A. Ahmed, J. V. Rushworth, N. A. Hirst, and P. A. Millner, *Microbiol. Rev.*, **27**, 631–46 (2014).
34. D. Bansi, A. Malhotra, Chaubey, and S. P. Singh, *Anal. Chim. Acta*, **578**, 59–74 (2006).
35. H. Shurvell, *Handbook of Vibrational Spectroscopy* (New York, Wiley) (2006).
36. P. K. Gupta, Z. H. Khan, and P. R. Solanki, *Electroanal. Chem.*, **829**, 69–80 (2018).
37. P. K. Gupta, P. P. Sharma, A. Sharma, Z. H. Khan, and P. R. Solanki, *Mater. Sci. Eng. B*, **211**, 166–72.
38. A. K. Yadav, T. K. Dhiman, G. Lakshmi, A. N. Berlina, and P. R. Solanki, *Int. J. Biol. Macromol.*, **151**, 566–75.
39. G. Lakshmi, A. Sharma, P. R. Solanki, and D. K. Avasthi, *Nanotechnology*, **27**, 345101 (2016).
40. F. A. G. Silva Jr, J. C. Queiroz, E. R. Macedo, A. W. C. Fernandes, N. B. Freire, M. M. da Costa, and H. P. de Oliveira, *Mater. Sci. Eng. C*, **62**, 317–22 (2016).
41. J. B. Terry, *J. Bacteriol.*, **15**, 4725–33 (1999).
42. D. Fortin, F. G. Ferris, and T. Beveridge, *J. Rev Mineral.*, **35**, 161–80 (1997).
43. N. Idil and B. Mattiasson, *Sensors (Basel)*, **17**, 708 (2017).